ASTR 3760 Solar and Space Physics Final Project

Kent L. Ritchie

University of Colorado Boulder, Spring 2019

Author Note

This final project is composed of my current research progress and future goals in the Solar Influences group supervised by Dr. Maria Kazachenko at the Laboratory for Atmospheric and Space Physics and National Solar Observatory in Boulder, Colorado. This is a mixture of a computational project and review paper per the final project guidelines as discussed previously with Professor Kazachenko.

Motivation for using my research as the ASTR 3760 final project subject: focus my understanding of the overall research goals, display instrumentation and solar physics course material overlapping with professional research, and to provide a detailed summary of research progress from the point of view of an undergraduate astrophysics student.

Purpose and Science Background

The main purpose of our research is to understand the relation between magnetic reconnection flux and solar flare intensity in different wavelengths and emission measures. This understanding will hopefully lead to scaling laws. Magnetic reconnection flux encompasses a great deal of information that we have discussed in the ASTR 3760 course including: plasma behavior, magnetohydrodynamics (MHD), Maxwell's equations, solar flares, coronal mass ejections (CME), and of course the solar magnetic field.

As learned in lecture, solar flare emissions occur from rapid conversion of free magnetic energy that is stored in the active region magnetic fields. Specifically, flare ribbons are the footprints of the reconnected flux tubes in the solar flare. The traditional flare model is the CSHKP (Carmichael 1964; Sturrock 1966; Hirayama 1974; Kopp & Pneuman 1976) model of two-ribbon eruptive flares. The Longcope (2007) schematic shows where reconnection occurs within the flare event. Three-dimensional MHD simulations of CMEs all produce something resembling the Longcope schematic. The important part of magnetic reconnection is that it cannot be measured directly from coronal observations; however, the CSHKP model does give a quantitative relationship between reconnection flux in the corona and the magnetic flux in the flare ribbon (Forbes & Priest 1984):

$$\frac{\partial \Phi}{\partial t} = \frac{\partial}{\partial t} \int B_c \, dS_c = \frac{\partial}{\partial t} \int B_{\mathrm{n}} \, dS_{\mathrm{ribbon}}$$

This relationship says the coronal magnetic reconnection rate as reconnection flux per unit time is the integrated value of inflow coronal magnetic field over the reconnection area. This normal component of the magnetic field refers to the flare ribbon magnetic field which is the footprint of newly reconnected magnetic field lines in the corona. The normal magnetic field component and

differential ribbon area are found via photospheric magnetogram and lower-atmosphere flare ribbon observations. A complex series of flare ribbon masking with Solar Dynamics Observatory (SDO) Atmospheric Imaging Assembly (AIA) completed by Kazachenko et al. 2017 supplies the calculated reconnection fluxes. All of this resulting flare ribbon data is made available in RibbonDB containing 3137 (April 2010 through April 2016) flare events of GOES class C1 and larger with heliographic longitudes of less than 45 degrees. The quantities included in RibbonDB include the following Heliophysics Event Catalogue (HEC) values: flare start, peak, and end times; peak x-ray flux; heliographic longitude and latitude; and active region number. Also included are the necessary observational values to compute the area-integrated quantities described above from the 160nm AIA image sequence.

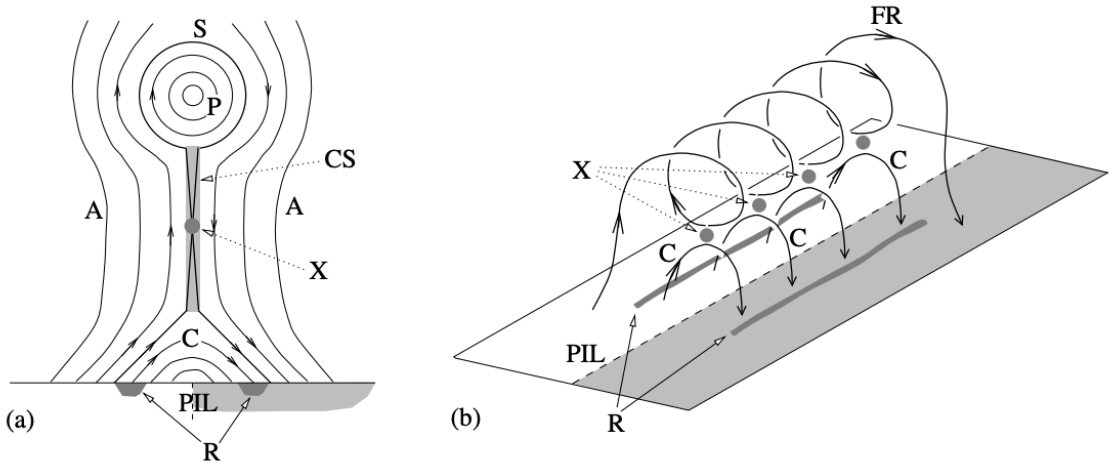

Figure 1: Basic elements of the CSHKP two-ribbon flare model in (a) two dimensions (2D; from Forbes 2000) and (b) three dimensions (3D; from Longcope et al. 2007). Here, 'R' indicates the location of the flare ribbons, 'CS' the current sheet, 'A' the overlying arcade, 'P' the erupting plasmoid, 'FR' the 3D flux rope, 'PIL' the polarity inversion line, 'X' the site(s) of magnetic reconnection, 'S' the separatrix boundary of the erupting CME flux rope, and 'C' the coronal flare loops formed by magnetic reconnection. Taken from Kazachenko et al. 2017.

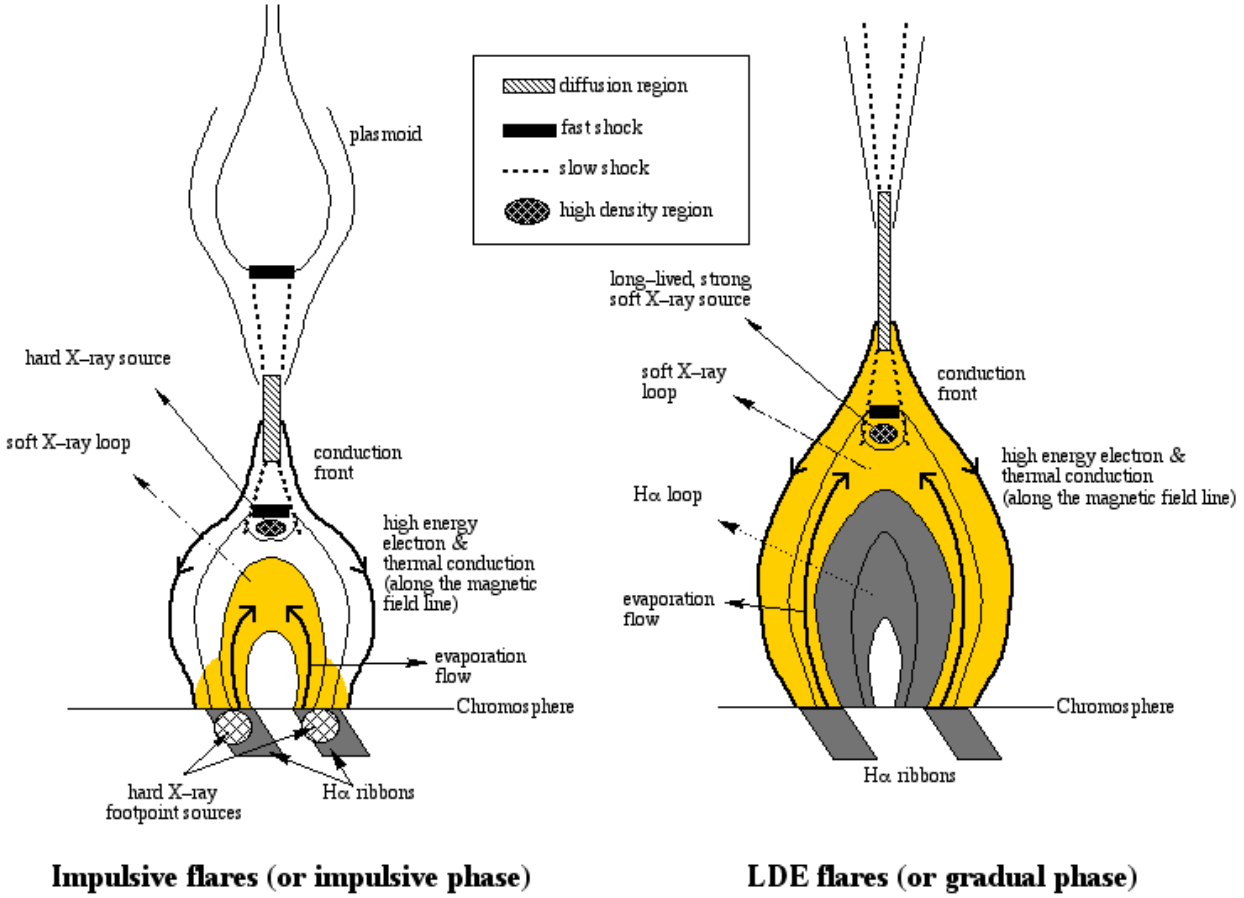

Figure 1: CSHKP model taken from Magara et al. 1996

My portion of the research uses RibbonDB reconnection flux and compares these values to available SDO Extreme Ultraviolet (EUV) Variability Experiment (EVE) data. SDO EVE measures the solar extreme ultraviolet (EUV) irradiance; specifically, it uses the Multiple EUV Grating Spectrograph (MEGS) that consists of a set of two Rowland-circle grating spectrographs covering the 5 – 105nm spectral irradiance range with a 0.1nm spectral resolution. Our research utilizes level 2 line data from the MEGS-A and MEGS-B channels of the instrument. The MEGS-A channel is a grazing incidence grating spectrograph with a measurement range of 5 – 37nm. The MEGS-B channel is a double normal-incidence grating spectrograph with a measurement range of 35 – 105nm. As of May 26, 2014, the MEGS-A detector is no longer active due to a capacitor short. MEGS-B has since been extended to its lowest wavelength of 33.5410nm. This limits the entirety of EVE line data (EVL) acquisition to three hours per day. Level 2 EVL data files available to the public for scientific or personal use are split into hourly FITS files. Within the individual FITS files, the header unit "LinesData" contains all of the actual science measurements for the observation period for lines, bands, and diodes. The line irradiance data is averaged over 10 seconds, without any background subtraction, giving a single irradiance value for each of the 39 emission lines. This is the data used in my research referred to as "flux data" from here on. The available lines from EVE are shown below in *Figure 3*.

Fe XVIII	9.39260	6.81000	0
Fe VIII	13.1240	5.57000	1
Fe XX	13.2850	6.97000	2
Fe IX	17.1070	5.81000	3
Fe X	17.7243	5.99000	4
Fe XI	18.0407	6.07000	5
Fe XII	19.5120	6.13000	6
Fe XIII	20.2044	6.19000	7
Fe XIV	21.1331	6.27000	8
He II	25.6317	4.75000	9
Fe XV	28.4150	6.30000	10
He II	30.3783	4.70000	11
Fe XVI	33.5410	6.43000	12
Fe XVI	36.0758	6.43000	13
Mg IX	36.8076	5.99000	14
S XIV	**44.5700**	**6.44000**	**15**
Ne VII	46.5221	5.71000	16
Si XII	49.9406	6.29000	17
Si XII	**52.1000**	**6.28000**	**18**
O III	52.5795	4.92000	19
He I	**53.7000**	**3.84000**	**20**
O IV	55.4370	5.19000	21
Fe XX	**56.7870**	**6.96000**	**22**
He I	58.4334	4.16000	23
Fe XIX	**59.2240**	**6.89000**	**24**
O III	59.9598	4.92000	25
Mg X	**60.9800**	**6.10000**	**26**
Mg X	62.4943	6.05000	27
O V	62.9730	5.37000	28
O II	71.8535	4.48000	29
Fe XX	**72.1560**	**6.96000**	**30**
Ne VIII	77.0409	5.81000	31
O IV	79.0199	5.19000	32
O II	**83.5500**	**4.52000**	**33**
H I	**94.9700**	**3.84000**	**34**
H I	97.2537	3.84000	35
C III	97.7030	4.84000	36
H I	102.572	3.84000	37
O VI	103.190	5.47000	38

Figure 3: EVE emission lines with line name, centered wavelength in nm, log10 temperature in K, and line number.

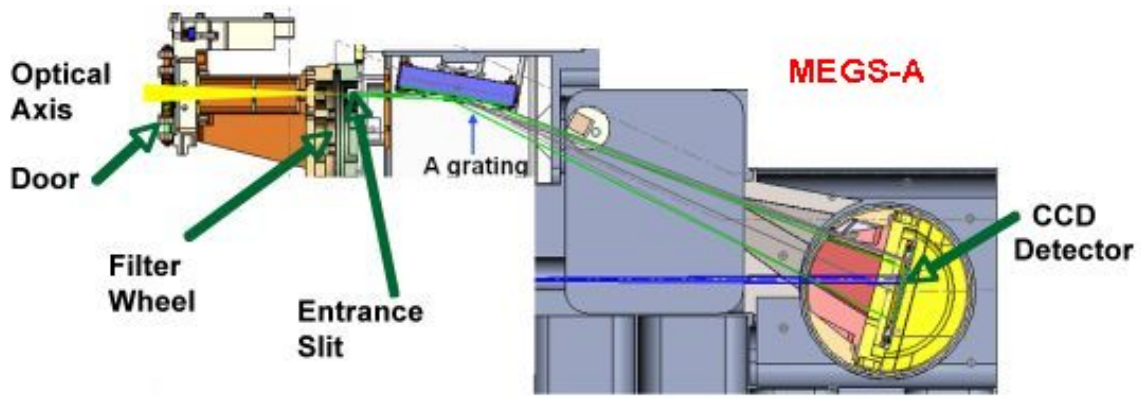

Figure 4: This picture shows the optical layout for MEGS-A. The solar radiation enters from the left, goes through foil filters and slit, and different wavelengths reflect / diffract off the spherical grating onto the CCD detector.

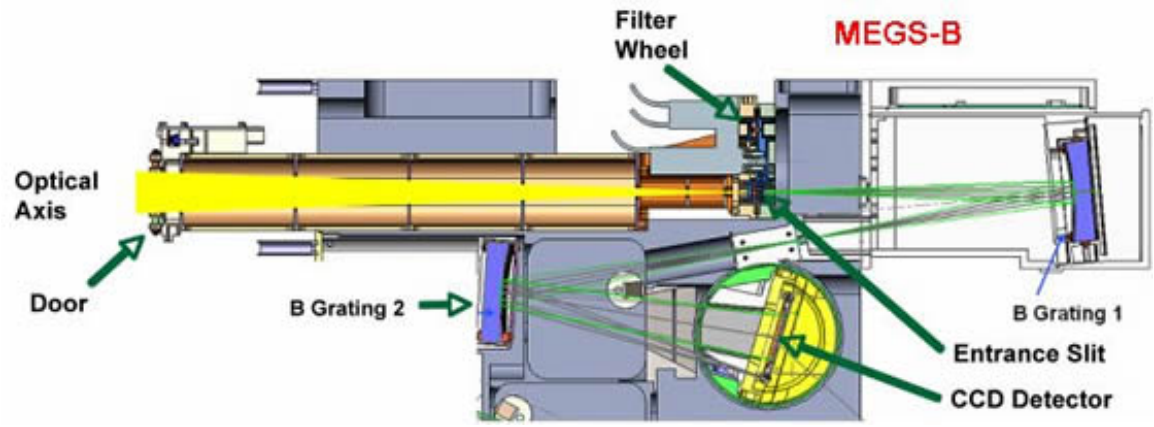

Figure 5: This picture shows the optical layout for MEGS-B. The solar radiation enters from the left, goes through an entrance slit, diffracts off the first spherical grating, goes through another slit, and then diffracts off the second spherical grating onto the CCD detector.

EVE was designed by LASP and the data is maintained by Dr. Don Woodraska and additional EVE Data Systems team members at LASP. I had the honorable opportunity to be part of this team from January – August 2018 and gained a unique amount of EVE instrumentation knowledge. Further instrumentation detail http://lasp.colorado.edu/home/eve/science/instrument/

Python Programming and Data Analysis

The flare ribbon catalogue RibbonDB, described in Kazachenko et al. 2017, contains the active-region and flare-ribbon properties of all flares of GOES class C1.0 and larger observed during the SDO era, from April 2010 until April 2016, containing 3137 total events. The RibbonDB events were compared to available EVE line data. Specifically, we compared total flux values and peak flux values during the duration of flare events in RibbonDB. This was accomplished through various scripts written in Python:

1. Download EVL data files for all hours included in RibbonDB events
2. Calculate 39 flux arrays for each RibbonDB event with EVL data files from Script 1 and save as .txt files
3. Calculate total flux and peak flux of each emission line for each RibbonDB event with background subtraction with flux arrays from Script 2 and save as .txt files
4. Plot EVL total flux versus RibbonDB reconnection flux for all 3137 RibbonDB events
5. Plot EVL peak flux versus RibbonDB reconnection flux for all 3137 RibbonDB events

The primary cause of difficulty has been in handling missing/corrupt data. There are many reasons data is missing/corrupt, but the most abundant reason is that MEGS-B only operates up to three hours per day. To minimize the degradation on the MEGS-B detector, MEGS-B only observes the sun two to three hours per day and the timing of the observation has changed throughout the mission. When not observing the sun, the MEGS-B portion of the spectra is filled with -1.0. The easiest fix was to change all -1.0 values to 0, this ensures that the total flux and peak flux values are not affected. An unfortunate effect from all this missing data is the need to throw out RibbonDB events that cannot be properly normalized with a background subtraction. A background subtraction was performed by using the flux value at the start time of the flare event as the

background value and subtracting that value from all flux values within the event time of the flare. A background subtraction is necessary because the flux value measured during a flare is the sum of the active region's quiet sun and the flare event which would give improper total flux values due to the flare event alone, thus we are subtracting out the active region's quiet flux value before the flare. Out of the 3137 total events in RibbonDB:

- 65% occurred prior to the anomaly of MEGS-A
- 35% occurred after the anomaly
- Overall, MEGS-B emission lines have 82% of data missing due to the limited observation time of three hours per day
- MEGS-A emission lines have 39% of data missing

This still leaves a large amount of flare events to be used in determining scaling laws between magnetic reconnection flux and total/peak flux. The next step in my research is to perform Spearman statistics to determine the exponential relations for specific emission lines that appear to have the most significant trends. Below are a few plots that are most promising in calculating these scaling laws.

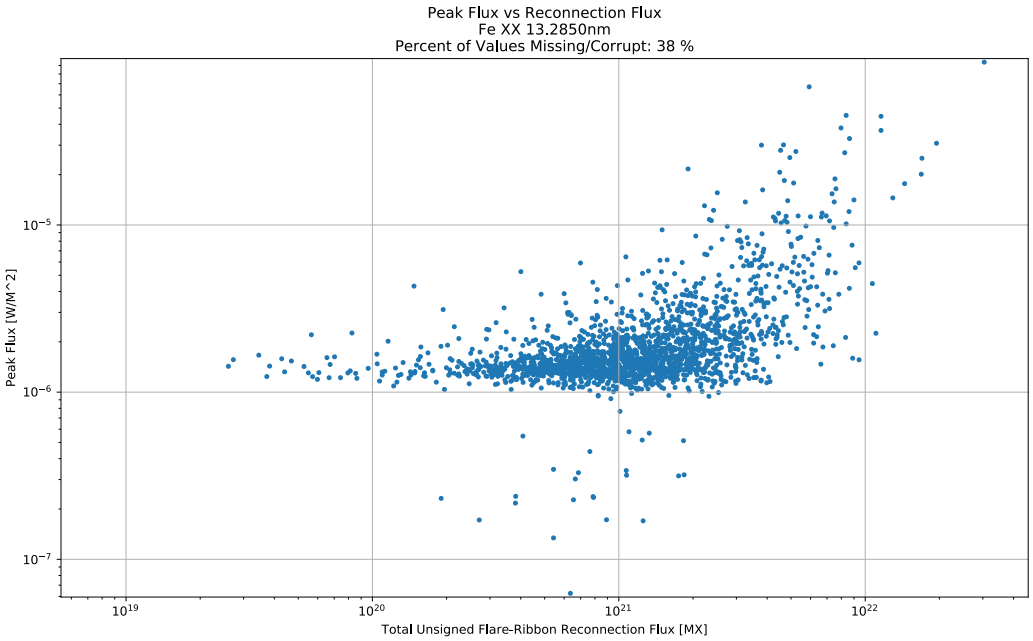

Figure 6: Peak flux vs reconnection flux for all available RibbonDB events with accurate background subtractions from EVL data for the Fe XX 13.2850nm emission line

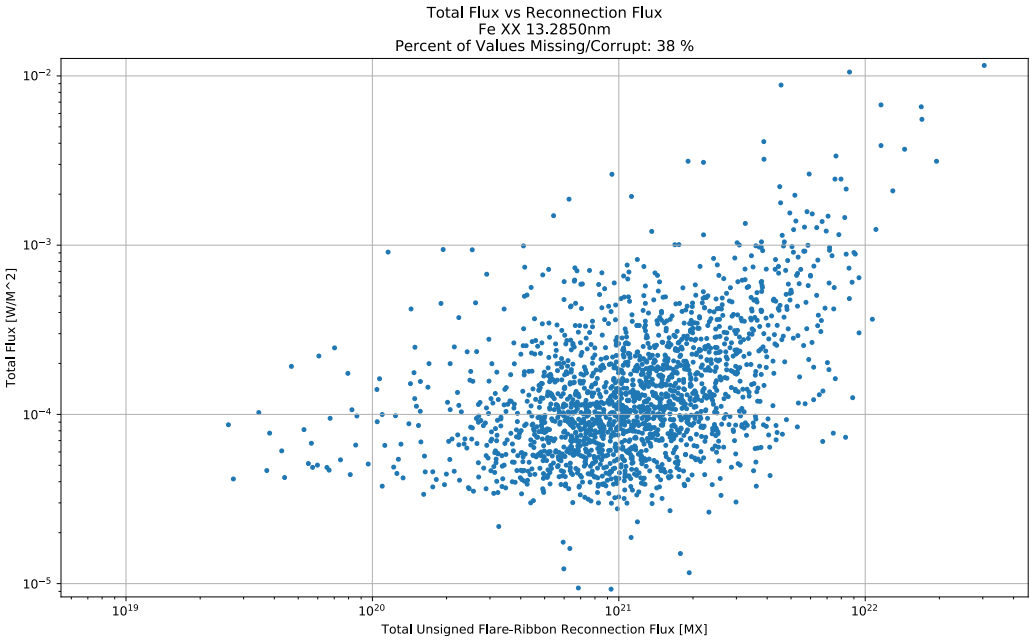

Figure 7: Total flux vs reconnection flux for all available RibbonDB events with accurate background subtractions from EVL data for the Fe XX 13.2850nm emission line

Conclusion

Having the opportunity to perform undergraduate research and take an undergraduate course in solar physics is extremely interesting and confirms my intent on professional research in the field after graduating. ASTR 3760 provided a great mixture of lecture material, homework sets, and extra reading assignments to ensure success in solar and space physics research. This course has motivated me to enroll in graduate level plasma physics as an undergraduate senior next spring. Studying and researching solar flares in the solar magnetic field has been gratifying with the abundance of new knowledge gained each day. My goals for this research project include publishing in the summer of 2019, presenting results at a conference or local talk, and making myself a competitive applicant for full-time solar physics research during the exciting emergence of The Daniel K. Inouye Solar Telescope (DKIST). I am thankful for the opportunities presented at CU that supply its students with unparalleled experience in research, instrumentation, and course work. I look forward to a career in solar physics.

Sources and References

Carmichael, H. 1964, NASA Special Publication, 50, 451

Forbes, T. G. 2000, J. Geophys. Res., 105, 23153

Hirayama, T. 1974, SoPh, 34, 323

Kopp, R. A., & Pneuman, G. W. 1976, SoPh, 50, 85

Longcope, D., Beveridge, C., Qiu, J., et al. 2007, SoPh, 244, 45

Magara, T., Mineshige, S., Yokoyama, T., & Shibata, K. 1996, ApJ, 466, 1054

Sturrock, P. A. 1966, Nature, 211, 695

RibbonDB: http://solarmuri.ssl.berkeley.edu/~kazachenko/RibbonDB/

SDO EVE: http://lasp.colorado.edu/home/eve/

SDO AIA: https://aia.lmsal.com/

ASTR 3760 materials: http://solarmuri.ssl.berkeley.edu/~kazachenko/ASTR_3760_2019/

Research project: https://github.com/astroritchie/eveproject